

# Effect of Nanographite on Electrical, Mechanical and Wear Characteristics of Graphite Epoxy Composites

Sanjeev K. Joshi<sup>#,\*</sup>, Ashavani Kumar<sup>\$</sup>, and M.G.H. Zaidi<sup>@</sup>

<sup>#</sup>DRDO HQr, DRDO Bhawan, Delhi-110 011, India

<sup>#\$</sup>Department of Physics, National Institute of Technology, Kurukshetra - 136 119, India

<sup>@</sup>Department of Chemistry, G.B. Pant University of Agriculture & Technology, Pant Nagar - 263 145, India

\*E-mail: [technology\\_advisor@hqr.drdo.in](mailto:technology_advisor@hqr.drdo.in)

## ABSTRACT

Effect of weight fraction (WF, mg/dL) of nanographite (NG, 400 nm) on electrical, mechanical and wear and characteristics of graphite epoxy composites (GECs) were investigated. For this purpose, a series of GECs was prepared through dispersion of various WF of NG into epoxy resin, followed by curing with polyamine. Dispersion of NG into epoxy matrix and onward formation of GECs and was revealed through Ultraviolet, Fourier transformed Infrared spectra and atomic force micrographs. Photoelastic analysis in combination with atomic force microscopy reveals the presence of uniformly dispersed domain of NG into stress free matrix of GECs with fringe order ranging 0.23 to 0.61 under compression of 8 to 20 kgf. GECs have rendered a rising trend in DC conductance ranging 98.32 nS/cm to 0.54  $\mu$ S/cm with electrical percolation threshold at 175 WF of NG. GECs have shown enhanced compressive, impact, tensile, strength, Rockwell hardness and wear resistance at 200WF of NG. In general, GECs has shown a marginal modification in their compressive strength by 5.30 % over cured epoxy (CE). However, impact (%) and tensile strengths (%) of GECs were largely improved to 31.78 and 43.98 over CE.

**Keywords:** Nanographite; Weight fraction; Spectra; Microstructure; Stress analysis; DC Conductance; Mechanical properties; Wear behaviour

## 1. INTRODUCTION

Epoxies are thermosetting networks derived through curing of oxirane functional monomers with organic acids, anhydrides or polyamines<sup>1</sup>. Epoxies have received wide scope of applications over decades with key example as electrical insulators, adhesives, coatings and structural materials<sup>1-3</sup>. However, inherent brittleness, high internal stress, limited toughness, impact strength<sup>4-9</sup> and losses in their mechanical stability under external stress and chemical environments has raised need of their modification through reinforcing carbonaceous, inorganic, polymeric and waste materials as fillers<sup>1-3,10</sup>.

Carbon presents the family of allotropes in diverse shapes, aspect ratios, physical properties and reactivity<sup>11</sup>. Graphite is the parent allotrope of carbon with layered graphene sheets held through *van der Waals* forces. High natural abundance, low cost, moderate electrical conductance and tunable surface area has raised the preference to graphite as filler for epoxy modification<sup>12</sup>. However, improper compatibility of graphite and dispersion into epoxy matrix leads to their agglomeration in epoxy matrix<sup>13</sup> that limits the electrical conductance<sup>14</sup>, impact strength<sup>15</sup>, fatigue<sup>16</sup>, tensile strength<sup>17</sup>, wear resistance<sup>17-18</sup> and chemical stability<sup>19</sup> of resulting graphite epoxy composites

(GECs). For such reasons, GECs finds their limited scope of application as conducting electrodes for fuel cells<sup>20-21</sup> and in development of chemical and biosensors<sup>22-23</sup>.

Recently, nanographite [NG] existing as graphite nanoplatelets has received growing attention as one dimensional nanofillers for epoxy modification<sup>24-26</sup>. NG is the novel class of carbonaceous material with high surface area at small lateral size. NG, due to their wide range of aspect ratios and ease of availability at a low cost are preferred over other carbonaceous nanofillers for development of polymer nanocomposites. NG differs from natural graphite in terms of ease of processability<sup>27-30</sup>, high binding affinity with epoxy resin (ER) and liquid curing agents like polyamines (PA)<sup>24-26</sup>. High surface area<sup>31</sup>, prominent electrical conductance<sup>32</sup> and ease of dispersion of NG into ER deliver polymer nanocomposites with improved mechanical properties and wear behaviour<sup>33-34,40-41</sup>. Such promising physical characteristics of NG makes them a promising filler for development of GECs with improved DC conductance<sup>35-36</sup>, mechanical properties<sup>37-41</sup> and wear resistance<sup>40-41</sup>. However, low weight fraction (WF, mg/dL) of NG are recommended for achieving enhanced dispersion and DC conductance of GECs, whereas high WF of NG results GECs with improved mechanical properties and wear resistance. While much progress has been made on development GECs, from naturally abundant graphite and its NG analogue up to 5WF<sup>4-9,13-14,18-22</sup>. The current manuscript

deals with additional explorations related to optimum WF of NG that could result GECs with improved mechanical properties, wear resistance, electrical conductance and reduced internal stress are yet to be made. The objective of present communication is to report the effect of WF of NG ranging 0 to 300 on their dispersion into CE and onwards modification in mechanical properties, wear resistance, internal stress and DC conductance of GECs.

## 2. EXPERIMENTAL

### 2.1 Materials

Epoxy resin (LY 556, density 1.16 g/cc) and polyamine hardener (PA, HY 951) were procured from Huntsman India Limited, NG with average particle size 400 nm, purity >99.5% was procured from SRL Chemicals India. Other chemicals and solvents with purity >99.5 % were locally arranged and used without purifications<sup>42</sup>.

### 2.2 Preparation of GECs

All preparations were conducted in a temperature controlled autoclave ( $\pm 1^\circ\text{C}$ ) with 316-stainless steel make reaction chamber of 125 mL capacity. GECs were prepared through slight modifications of method reported earlier<sup>42,43</sup>. In brief, a suspension of epoxy resin (ER, Epoxy equivalent 196 g/ equivalent) supplemented with requisite WF of NG was subjected to ultrasonication over 10 min at 500W followed by thermal activation at  $90 \pm 1^\circ\text{C}$  over 1h and curing with PA (15%, v/v) at  $40 \pm 1^\circ\text{C}$ . In order to have the GECs free from air pockets, prior to curing, thermally activated suspensions were kept under evacuation at 400 mm Hg/ $40 \pm 1^\circ\text{C}$  over 20 min. Cured GECs were kept over a week under evacuation at 400 mm Hg/ $25 \pm 1^\circ\text{C}$ , thereafter post cured under a domestic MW oven 25W over 10 min. A sample of cured epoxy (CE) was also fabricated under identical conditions and served as control.

### 2.3 Characterisation

All the procedures involving characterisation of samples has been adopted from the procedures reported earlier and are briefly re-described<sup>42</sup>. Ultraviolet (Uv) spectra were recorded over Genesis-10Thermospectronic Spectrophotometer in a formulation of acetone (20%,v/v) in N-methyl pyrrolidone (NMP). FT-IR spectra were recorded in transmission mode on Perkin Elmer FTIR spectrophotometer in KBr. Height images were recorded over NTEGRA Prima atomic force microscope (AFM) under tapping mode using ultra sharp Si cantilevers having force constant of 48 N/m at room temperature<sup>44</sup>. DC conductance of samples was recorded through four probe method at  $35 \pm 1^\circ\text{C}$  over Keithley Nanovoltmeter model 2182 A coupled with 6221 current source and an indigenous sample holder with PID controlled oven. Two parallel surfaces of each sample apart from 1 mm were polished with sand paper followed by silver paint and checked for good electrical conduction<sup>43</sup>.

Mechanical characterisations were made according to ASTM D recommendations (Table 1). Tensile strength was

**Table 1. Effect of WF of NG on electrical, mechanical and wear behaviour of GECs**

	ASTM D	WF (mg/dL) of NG			
		0	100	200	300
DC conductivity $\times 10^{-3}$ ( $\mu\text{S}/\text{cm}$ )			0.42	0.52	0.53
Tensile strength (MPa)	638	30.36	38.60	42.70	43.70
Elongation (%)		18.87	18.14	11.55	10.49
Compressive strength (MPa)	695	130.70	131.36	136.92	137.64
Impact strength (KJ/m <sup>2</sup> )	256	17.15	18.32	21.84	22.60
Hardness (R-Scale)	785	74.90	84.40	91.67	93.60
Wear loss ( $W_L$ ) at 2.0 bar		3.70	3.59	3.55	3.39
$W_L$ at 4.0 bar		3.99	3.72	3.67	3.58

recorded at cross head speed of 1.0 mm/min over computer controlled Tesnometer<sup>17</sup>. Compressive strength was recorded @ 5.0 mm/min on Tenuous Olsen universal testing machine with capacity of 35 KN. Izod Impact strength was recorded using notched specimens fabricated at 0.001 mm accuracy of screw gauge and venire caliper. Rockwell hardness was recorded with ball indenter ( $\frac{1}{2}$ " , 12. 70 mm) at minor load of 10 kgs<sup>15</sup>.

Wear behaviour was investigated on Plint wear and friction machine equipped with dead weight tester, transducer (calibrated at 0.892 mv/v) and a chart recorder. The machine was coupled with lathe for carrying a disc shaped specimen on a mandrel. This was connected with two pins pressed into contact at opposite surfaces of the disc by means of hydraulic cylinders. Hydraulic end load was applied by means of a precision weight pressure tester, loaded with arbitrary dead weights. A conical hole, with included angle of  $60^\circ$  and of 5 mm diameter was drilled at the end face of the pins. Elapsed time and the cumulative number of revolutions were recorded from digital counter equipped with the panel. Wear rate was estimated through differential weighing of the mass of pin at accuracy of 1 mg, at the intervals of 60 s<sup>17</sup>. Photoelastic analysis was conducted over standard circular polariscope irradiated in monochromatic light. Stress analysis data was recorded under diametric compression of circular disc shaped specimens of 75 mm diameter and 5 mm thickness at 4 to 20 kgf<sup>5</sup>.

## 3. RESULTS AND DISCUSSION

### 3.1 Spectra

Figure 1 presents the absorption maxima of individual reactants and their shift on event of the formation of products. ER and PA have shown their individual absorption maxima at 282 and 294 nm. Curing of ER with PA results CE with absorption maxima at 288 nm. Shift in absorption maxima from 282 to 288 attributes to formation of  $-\text{OH}$  and  $-\text{NH}-$  as auxochromic pairs on event of curing of ER with PA<sup>42</sup>. NG and a representative GECs synthesised at 300 WF of NG renders common absorption maxima at 246 nm that attributes to presence of graphitic domains into the matrix of GECs. An additional absorption maxima corresponding to GECs was appeared at 291 nm. Graphitic materials are associated with inherent oxygen bearing groups that makes them reactive

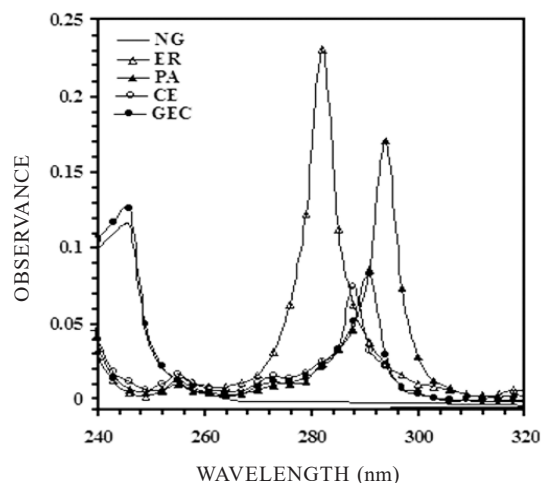


Figure 1. Ultraviolet Spectra nanographite (NG), epoxy resin (ER), polyamine (PA), cured epoxy (CE) and GEC Prepared at 300 WF of NG.

with molecules of different functionalities<sup>25-26</sup>. In the present investigation, appearance of optical maxima at 291 nm attributes to the formation of GECs through reaction of oxygen bearing groups of NG with oxirane functionalities during the process of curing of ER with PA.

Further insight into presence of oxygen bearing functionalities over NG, formation of CE and respective GECs was made through wave numbers ( $\text{cm}^{-1}$ ) appeared in FTIR spectra (Fig. 2). CE has shown characteristic wave numbers at 3670.25 ( $\nu$  O-H), 1756.23 ( $\nu$  C=O), 1673.27 ( $\delta$ N-H), 1457.09 ( $\delta$ C-H), and 749.88 (oxirane ring) (2a)<sup>42</sup>. Residual oxygen bearing functionalities introduced during the manufacturing of NG were appeared at 2924 ( $\nu$  O-H), 2846 ( $\nu$  C-H), 1632 ( $\nu$  C=O) and 1110 ( $\delta$  O-H). Additionally, NG shows the characteristic functionalities of graphene derived C=C at 1345 to 1710. GECs synthesised at 300 WF of NG (2c) have shown a large resemblance with NG in the wave number range of 4000 to 2270 (2b) with simultaneous reduction in transmittance over CE (2a). Characteristic wave numbers associated with CE (2a) falling in the range of 2270 to 1400 ( $\nu$  C=O,  $\delta$  N-H,  $\delta$  C-H) and 1345 to 1710 (graphene derived C=C) were reappeared in GECs (2c). Moreover, the transmittance at wave numbers associated with graphene derived C=C

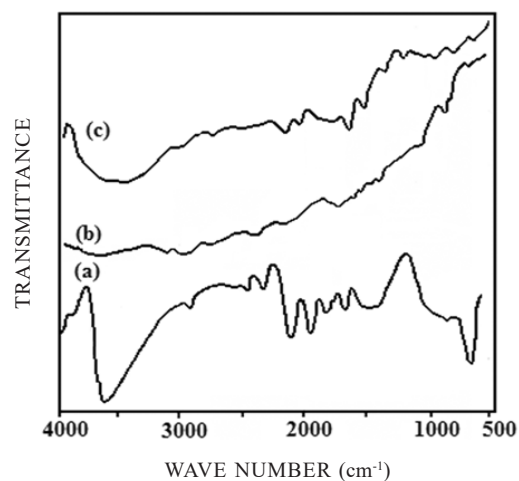


Figure 2. FTIR Spectra of (a) CE, (b) NG and (c) GECs synthesised at 200 WF of NG.

falling in the range of 1345 to 1710 (2b) found intensified in GECs (2c). Such increase of transmittance in the range of graphene derived C=C attributes to enhanced enrichment of NG into GECs. Results based on spectral analysis reveals that residual oxygen bearing functionalities over NG plays constructive roles in their integration with macromolecular segments of CE produced during the process of curing with PA<sup>28,42</sup>.

### 3.2 Microstructure

Figure 3 presents atomic force micrographs (AFM) of CE (a), representative GECs synthesised at 20 (b) and 200 WF of NG (c) at the XY stage of 5  $\mu\text{m}$ . AFM reveals biphasic composition of GECs with bright zones corresponding to prominence of NG, and small entities with grains identifiable as ordered domains of CE, forming dark phase. The inherent properties of the phases were related to their relative phase contrast. Brighter areas of AFM images attributes to greater force experienced by the cantilever tip during contact with NG. CE has shown characteristic phase separated morphology with average roughness of 47 nm at the depth of 149 nm (Fig. 3a). However, GECs were found free from the aggregates of NG (Fig. 3b). This reveals that at low WF, GECs with qualitatively improved dispersion of NG were

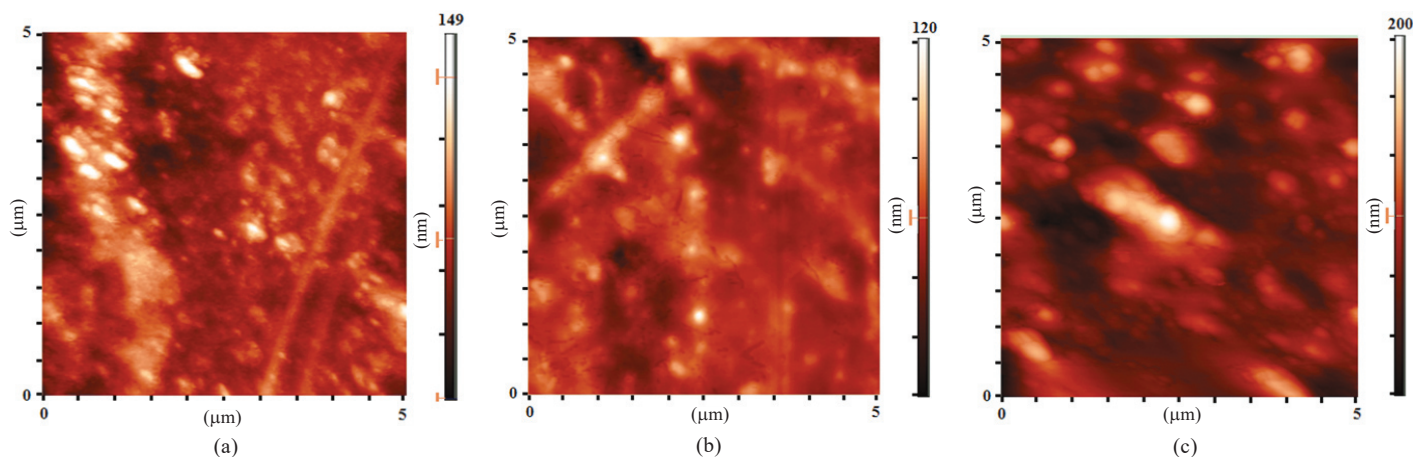


Figure 3. (a) AFM of CE, (b) AFM of GECs Synthesised at 20 WF of NG, and (c) AFM of GECs Synthesised at 300 WF of NG.

produced<sup>42</sup>. NG at 200 WF has demonstrated the persistent tendency of clustering into agglomerates. (Fig. 3c). The extent of relative changes in morphology of GECs was further explored through examination of their average roughness ( $a_r$ , nm). CE shows average roughness ( $a_r$ , nm) of 26.45 at the depth (nm) of 149 (Fig. 3b). With WF of NG, gradual increase in the ar of respective GECs was observed. GECs with 20 WF of NG has rendered the ar of 9.06 at the depth of 120 nm (Fig. 3b). An increase in  $a_r$  to 89.55 nm at the depth of 200 nm was observed for GECs with 200 WF of NG (Fig. 3c). AFM based microstructural examinations reveals that low WF down to 20 was found most effective in achieving improved dispersion of NG into matrix of CE<sup>44</sup>.

**3.3 Photoelastic Behaviour**

Photoelastic measurements are known over decades as non-contact and non-destructive method of real-time stress analysis during damage and repair of transparent polymers, complex pore structures and related composite materials<sup>47</sup>. Although, epoxies are known for their photoelastic behaviour, a few reports has been documented in relation to photoelastic behaviour of epoxy based nanocomposites.<sup>43</sup>. Experimental stress analysis evaluates isochromatic fringe order defined as the number of fringes that pass through the point under application of external loads. In the present investigation, effect of WF of NG on fringe order of GECs was investigated under diametric compression of disc shaped specimens ranging 4 to 20 kgf<sup>4</sup>. Present studies reveals that GECs with WF ranging 1.0 to 20 has rendered fringe order ranging 0.23 to 0.61 under diametric compression ranging 8 to 20 kgf<sup>43</sup>. However, no distinct fringe order was appeared up to the diametric compression of 4.0 for all the samples synthesised over 20WF of NG (Fig. 4). In general, all GECs have regained their initial mechanical properties along with specimen dimensions, and display a complete release of the

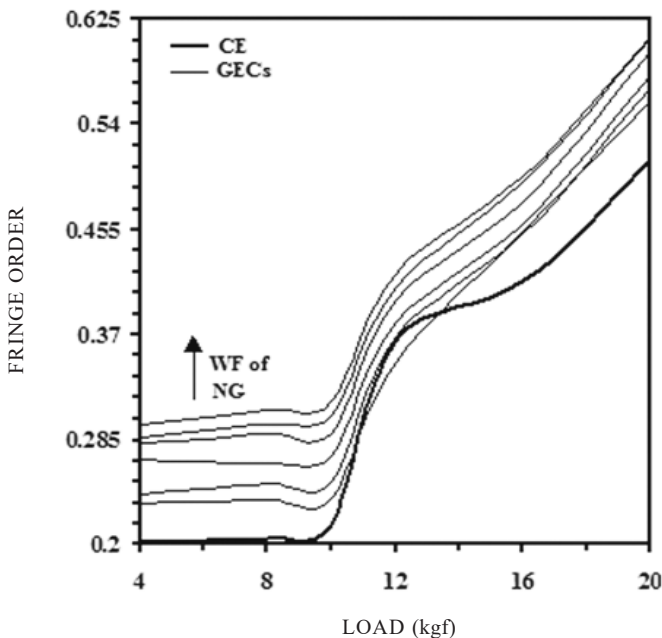


Figure 4. Effect of WF of NG ranging 1.0 to 20 on photoelastic behaviour of GECs.

residual stress through transfer to cured epoxy matrix during the diametric compression<sup>6-8</sup>.

**3.4 Electrical Conductance**

In order to have insight into the dispersion of the NG into CE, DC conductance of GECs was investigated. Transitions from insulator to conductor are explained in terms of percolation threshold value. An electrical percolation threshold is the minimum quantity of conductive filler associated with electrical conductance of the composite from insulator to conductive phase<sup>14</sup>. DC conductance measurements were conducted under two different set of WF of NG (Fig. 5). The first part of study comprises conductance measurements ranging 100 to 300 WF of NG. Such high WF of NG was assigned due to low in plane DC conductance of GECs. However, in plane DC conductance of GECs could be improved through incorporation of large amount of conductive filler to achieve the desired level of DC conductance<sup>45</sup>. Another section comprise conductance measurements up to 20WF of NG (Fig. 5). High WF of NG ranging 100 to 300, impart rise in the electrical conductance ( $\mu\text{S}/\text{cm} \times 10^{-3}$ ) of GECs ranging 0.42 to 0.53, that was optimised at 0.53 with an electrical percolation threshold at 175 WF of NG (Fig. 5a). Such high DC conductance at WF of NG ranging 100 to 200 attributes to formation of electrical conducting pathways into GECs<sup>35-36</sup>. NG up to 20WF imparts gradual rise in Dc conductance (nS/cm) ranging 98.32 to 119. (Fig. 5b). Increase in voltage up to 100V imparts no significant improvement in Dc conductance, that attribute to electrical insulation in GECs<sup>32,42-43</sup>. Such enhanced electrical conductance of GECs derived at low WF of NG is being driven due to increase in excluded-volume associated with high aspect-ratios of NG<sup>42-43</sup>.

**3.5 Mechanical Properties**

Table 1 demonstrates the effect of WF of NG ranging 0

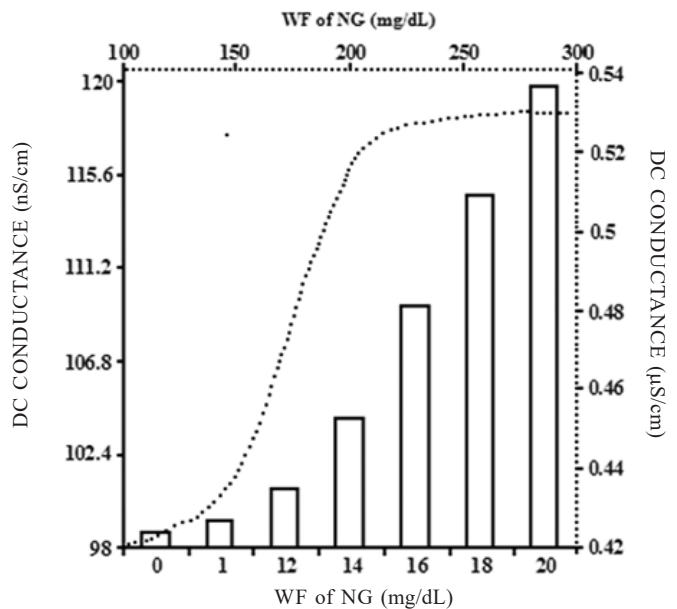
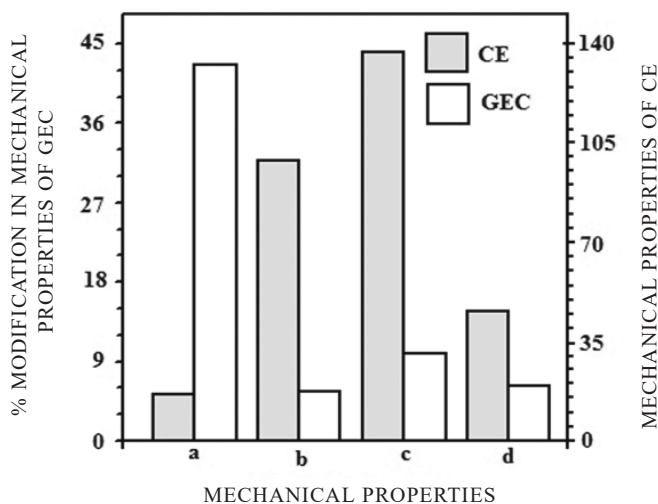


Figure 5. DC conductance of GECs synthesised at (a) low WF of NG ranging 0 to 20 (Bar diagram) and high WF of NG (dotted lines).

to 300 on tensile behaviour, compressive and impact strength of GECs. The ultimate modification (%) in the various mechanical properties over CE is sketched in Fig. 6. In general, mechanical properties of GECs were largely improved up to 100 WF of NG. Further increase in WF of NG to 200 has raised the mechanical properties of GECs to maximum and was marginally improved with onward increase in WF of NG to 300. With WF of NG, tensile strength (MPa) of CE was raised from 30.35 to 42.7 and was stagnated to 43.70 till 300 WF of NG. GECs have shown an ultimate modification in tensile strength over CE by 43.98 per cent<sup>45</sup>. Modification in tensile strength was associated with simultaneous reduction in the elongation (%) by 14.76 over CE<sup>17</sup>. Such modification in tensile behaviour attributes to the inherent brittleness of GECs<sup>4</sup>. Accordingly, impact strength of CE was optimised to 21.84 at 200 WF of NG. Increase in WF of NG to 300 imparts a marginal increase in impact strength by 22.60 with ultimate improvement by 31.78 % over CE. However, increase in WF of NG to 300 imparts marginal improvement in compressive strength of GECs by 5.30 % over CE<sup>37-39,41</sup>.



**Figure 6. Comparative modification in various mechanical properties of GECs with reference to CE (a) Compressive strength (MPa), (b) Impact strength (kJ/m<sup>2</sup>), (c) Tensile strength (MPa), and (d) Elongation (%).**

Carbonaceous fillers are the major source of energy dissipation in polymer nanocomposites through mechanism of load transfer from filler to macromolecular segments. Mechanism of stress transfer prevails through segmental movements among macromolecular segments that specially increase the fracture energy of nanocomposites. Presence of oxygen bearing functionalities promotes the fortification of NG with macromolecular segments of CE (Fig. 2)<sup>37-39,42-43</sup>. In the present investigation, a rapid improvement in mechanical properties till 200 WF of NG attributes to fast transfer of load under elongation, compression or impact over GECs from relatively soft epoxy matrix to the strong NG filler.

### 3.6 Wear Behaviour

Resistance of GECs against wear depends on dispersion of NG their integration with epoxy matrix and Rockwell hardness (RH). NG bearing functionalities are compatible

with CE that imparts control over wear rate of GECs<sup>17-18,41</sup>. In the present investigation, effect of WF of NG on wear rate of GECs at hydraulic end loads (bar) of 2.0 and 4.0 under constant disc speed of 320 rpm was investigated. With WF of NG, a remarkable reduction in wear rate of GECs was observed irrespective to the applied hydraulic end load. Increase in hydraulic end load from 2bar to 4bar has enhanced the wear rates of GECs<sup>14</sup>. Wear of CE was progressed @ 3.70 mg/min at 2b that was gradually reduced to 3.55 mg/min at 200WF of NG (Table 1). GEC with 200WF has shown a marginal increase in wear rate to 3.66 at 4 bar. Study reveals that NG at 200 WF enhanced RH to GECs that imparts control over their wear rate up to 4bar at 232 rpm (Fig. 4). Such reduction in wear behaviour with improved RH hardness attributes to the formation of NG epoxy interface with improved strength<sup>17-18</sup>.

## 4. CONCLUSIONS

Effect of WF of NG ranging 0 to 300 on modification in mechanical properties, DC conductance and wear resistance of GECs was systematically investigated. Formation of GECs was revealed through diverse spectral methods, AFM and stress analysis. With WF of NG, DC conductance of GECs was increased ranging 99.32 nS/cm to 0.53  $\mu$ S/cm at 100V. GECs prepared up to 20 WF of NG were found with improved dispersion of NG into epoxy matrix. This has liberated GECs with reduced internal stress and photoelastic fringe order ranging 0.23 to 0.61 under diametric compression of 8 to 20 kgf. However, higher WF of NG ranging 100 to 300 has raised the DC conductance, mechanical stability and wear resistance to GECs. Study concludes that stress free GECs with desired durability and physical properties may be achieved through processing under optimised WF of NG. This may deliver the GECs suitable as material of construction for development of mechanically durable structures, conducting electrodes, optomechanical devices wear and resistant runways.

## REFERENCES

1. Khan, A., Bhawani, S. A. Asiri, A. M. & Khan I. Thermoset Composites: Preparation, properties and applications. *Material Research Forum*, U.K., 2018. 350p. doi:10.21741/9781945291876
2. Kocsis, J.K. & Kéki, S. Review of progress in shape memory epoxies and their composites. *Polymers* (Basel), 2018, **10**(1), 34-39. doi:10.3390/polym10010034
3. Zhang, Z.; Zhao N. & Hea, C. The superior mechanical and physical properties of nanocarbon reinforced bulk composites achieved by architecture design—a review. *Prog. Mater. Sci.*, 2020. doi:10.1016/j.pmatsci.2020.100672
4. Yang, J.U.; Zhangyu, R.; Lingtao, M. & Chiang, F. Quantitative visualization of the continuous whole-field stress evolution in complex pore structures using photoelastic testing and 3D printing methods. *Optics Express*, 2018, **26**(5), 6182. doi: 10.1364/OE.26.006182W
5. Colla, C. & Gabrielli, E. Photoelasticity and DIC as optical techniques for monitoring masonry specimens under mechanical loads. *In* Proceeding of IOP Conf. Series: J. Phy. 778, 2017, 012003.

- doi:10.1088/1742-6596/778/1/012003
6. Baptista, R.; Mendão, A. & Mendes, R. An experimental study on mechanical properties of epoxy-matrix composites containing graphite filler. *Procedia Struct. Integr.*, 2016,1,74-81.  
doi: 10.1016/j.prostr.2016.02.011
  7. Nisar, J.A.; Soutis, C. & Jones, F.R. Photoelastic analysis of stress transfer from matrix to fibre through an interphase in compression. *In* Proceeding of 12-th Conference of Aerospace Science & Aviation Technology, Cario, Egypt 2007. doi:10.21608/asat.2007.23990
  8. Jones, I.A.; Truman, C.E. & Booker, J.D. Photoelastic investigation of friction and residual stress in shrink-fitted shafts and hubs. *Appl. Mech. Mater.*, 2004, 1-2, 171-178. doi:10.4028/www.scientific.net/AMM.1-2.171
  9. Goodman, Sidney H. Epoxy Resins. *In* Handbook of Thermoset Plastics (Second Edition), Edited by Hanna Dodiuk Elsevier Science,1998, pp193-268.  
doi: 10.1016/B978-081551421-3.50009-6
  10. Jacob, S.; Lim, K.; Gan, C. L. & Hu, X.M. Unraveling the mechanistic origins of epoxy degradation in acids. *ACS Omega*, 2019, **4**, 10799–10808.  
doi: 10.1021/acsomega.9b00859
  11. Tiwari, S.; Kumar, V.; Huczko, A.; Oraon, R.; Adhikari, D. & Nayak, A.G. Magical allotropes of carbon: Prospects and applications. *Crit. Rev. Solid State Mater. Sci.*, 2015, **41**, 257-317. doi:10.1080/10408436.2015.1127206
  12. Gilardi, R.; Bonacchi D. & Spahr, M.E. Graphitic carbon powders for polymer applications *In* Filler for Polymer Applications, Edited by S. Palsule, Springer International Publishing, 2016. doi:10.1007/978-3-319-28117-9\_33
  13. Eric, S.W.K.; Susanna, M. L. & Howard, G. N. Physical aging in graphite/epoxy composites. *Polymer Composites*, 1982, **3**(1), 29-33. doi: 10.1002/pc.750030106
  14. Stabik, J. & Dybowska A. Electrical and tribological properties of gradient epoxy-graphite composites. *J. Ach. Mater. Manuf. Eng.*, 2008, **27**(1). 4.
  15. Derusova, D.A.; Vavilov, V.P.; & Druzhinin, N.V. Evaluating impact damage in graphite epoxy composite by using low-power vibrothermography. *In* Conference Proceeding, Thermosense: Thermal Infrared Applications XXXVIII, 2016, Society of Plastic Engineers, 98610F. doi:10.1117/12.2222987.
  16. Saunders, D. S.; Galea, S. C. & Deirmendjian, G.K. The development of fatigue damage around fastener holes in thick graphite/epoxy composite laminates. *Composites*, 1993, **24**(4), 309–321.  
doi: 10.1016/0010-4361(93)90041-6
  17. Bheemappa, S.; Ramesh, B.; Subbaya, K. & Chandramohan, G. Mechanical and three-body abrasive wear behavior of carbon-epoxy composite with and without wraphte filler. *J. Composite Mater*, 2010, **44**, 2509-2519. doi: 10.1177/0021998310369589
  18. Kumar, N.; Dash, S.; Tyagi, A.K. & Raj, B. Super low to high friction of turbostratic graphite under various atmospheric test conditions. *Tribology International*, 2011, **44**(12), 1969–1978.  
doi: 10.1016/j.triboint.2011.08.012
  19. Kaelble, D.H.; Dynes, P. J.; Crane, L.W. & Maus L. Interfacial mechanisms of moisture degradation in graphite-epoxy composites. *Journal Adhesion*, 2007, **25**-54.  
doi: 10.1080/00218467508078896.
  20. Ling, D. & Jana, S.C. Highly conductive epoxy/graphite composites for bipolar plates in proton exchange membrane fuel cells. *J. Power Sources*, 2007, **172**(2), 734-741.  
doi: 10.1016/j.jpowsour.2007.05.088
  21. Suherman, H.; Sahari, J.; Sulong, A. B.; Astuti, S. & Septe, E. Properties of epoxy/carbon black/graphite composites for bipolar plate in polymer electrolyte membrane fuel cell. *Adv. Mater. Res.*; 2014, **911**, 8–12.  
doi: 10.4028/www.scientific.net/amr.911.8
  22. Pividori, M.I.; Merkoçi, A. & Alegret, S. Graphite-epoxy composites as a new transducing material for electrochemical genosensing. *Biosensors Bioelectronics*, 2003, **19**(5), 473-84.  
doi:10.1016/S0956-5663(03)00222-7
  23. Serra, N.; Maeder, T. & Ryser, P. Piezoresistive effect in epoxy-graphite composites. *Sensors Actuators A: Physical*, 2012, **186**, 198-202. doi: 10.1016/j.sna.2012.04.025.
  24. Liu, S.; Venkata, S.C.; Xu, Z, Hui, D. & Wang, H. A review of extending performance of epoxy resins using carbon nanomaterials. *Composites Part B: Eng.*, 2018, **36**(1), 197-214. doi: 10.1016/j.compositesb.2017.08.020
  25. Kausar, A.; Anwar, Z. & Bakhtiar, M. Recent developments in epoxy/graphite, epoxy/graphene and epoxy/graphene nanoplatelet composites: A comparative review. *Polym. Plast. Tech. Eng.*, 2016, **55**, 1192-1210. doi: 10.1080/03602559.2016.1163589
  26. Kuzhir, P.A.; Paddubskaya, A.; Plyushch, N.; Volynets, I. S.; Maksimenko, J.; Macutkevici, I.; Kranauskaite, B.; Ivanov, J. E.; Kotsilkova, R.; Celzard, A.V.; Fierro, J.; Zicans, T.; Ivanova, R.; Meri, M.; Bochkov, I.; Cataldo, A.; Micciulla, F.; Bellucci, S. & Lambin, P. Epoxy composites filled with high surface area-carbon fillers: Optimization of electromagnetic shielding, electrical, mechanical, and thermal properties. *J. Appl. Phys.*, 2013, **114**, 164304. doi: 10.1063/1.4826529
  27. Al Sheheri, S. Z.; Al-Amshany, Zahra M.; Al Sulami, Q. A.; Tashkandi, N.Y. Hussein, M.A. & El-Shishtawy, R.M. The preparation of carbon nanofillers and their role on the performance of variable polymer nanocomposites, *Des. Monomers Polym.*, 2019, **22**(1), 8-53. doi: 10.1080/15685551.2019.1565664.
  28. Krishnamurthy, G.; Namitha, R. Synthesis of structurally novel carbon micro/ nanospheres by low temperature-hydrothermal process. *J. Chil. Chem. Soc.*, 2013, **58**(3), 1930-1933. doi: 10.4067/S0717-97072013000300030.
  29. Blomquist, N.; Engström, A. Christine.; Magnus, Hummelgård.; Andres, Britta.; Forsberg, Sven. & Olin, H. Large-scale production of nanographite by tube-shear exfoliation in water. *PLOS One*, 2016, **11**, 4.  
doi: 10.1371/journal.pone.0154686.
  30. Yu, V.; Ioni, S. V.; Tkachev, N.; Bulychev, A. & Gubin, S.P. Preparation of finely dispersed nanographite. *Inorganic*

- Materials*, 2011, **47**(6), 597–602.  
doi: 10.1134/S0020168511060100
31. Bellucci, S.; Micciulla, F.; Levin, V. M.; Petronyuk, Y. S.; Chernozatonskii, L. A.; Kuzhir, P.; Paddubskaya, A. G.; Macutkevic, J.; Pletnev, M. A.; Fierro, V. & Celzard, A. Microstructure, elastic and electromagnetic properties of epoxy-graphite composites. *AIP Advances*, 2015, **5**, 067137. doi: 10.1063/1.4922872.
  32. Wakabayashi, K.; Fujita, M.; Ajiki, H. & Sigrist, M. Electronic and magnetic properties of nanographite ribbons. *Physical Review B*, 1999, **59**(12), 8271–8282. doi: 10.1103/PhysRevB.59.8271
  33. Vidal, F.A.C. & Avila, F.A. Tribological investigation of nanographite platelets as additive in anti-wear lubricant: A Top-Down Approach. *Journal Tribology*, 2014, 136/031603-1 to 031603-9. doi: 10.1115/1.4027479
  34. Huang, H.D.; Tu, J.P.; Gan, L. P. & Li, C. Z. An Investigation on tribological properties of graphite nanosheets as oil additive. *Wear*, 2006, **261**(2) 140–144. doi:10.1016/j.wear.2005.09.010
  35. Chen, G.H.; Wu, D.J.; Weng, W.G. & Yan, W. L. Dispersion of graphite nanosheets in a polymer matrix and the conducting property of the nanocomposites. *Polym. Eng. Sci.*, 2001, **41**(12), 2148–2154. doi: 10.1002/pen.10909.
  36. Tirumali, M.; Balasubramanian, K. & Kumaraswamy, A. Functionally layered graphite reinforced epoxy composite sandwiched between epoxy composites: Their electrical and flexural properties. *Material Focus*, 2017, **6**(6), 691–697. doi: 10.1166/mat.2017.1467
  37. Mostovoy, S. & Yakovlev, A. V. Reinforcement of epoxy composites with graphite- graphene Structures. *Scientific Reports*, 2019, **9**, 16246. doi: 10.1038/s41598-019-52751-z
  38. Mamani, A.; Ebrahimi, M. & Ataefard, M. A study on mechanical, thermal and flame retardant properties of epoxy/expandable graphite composites. *Pigment Resin Tech.*, 2017, **46**(2), 131–138. doi: 10.1108/PRT-11-2015-0112
  39. Yasmin, A. & Daniel, I.M. Mechanical and thermal properties of graphite platelet/epoxy composites. *Polymer*, 2004, **45**(24), 8211–8219. doi: 10.1016/j.polymer.2004.09.054
  40. Prabhakar, K. ; Debnath, S.; Ganesan, R. & Palanikumar, K. A review of mechanical and tribological behaviour of polymer composite materials. *In Proceeding of IOP Conference Ser, Mater. Sci. & Eng.*, 2018, **344**. 012015. doi:10.1088/1757-899X/344/1/012015
  41. Agunsoye, J.O.; Bello, S.A.; Bello, L. & Idehenre, M.M. Assessment of mechanical and wear properties of epoxy-based hybrid composites. *Adv. Prod. Eng. Manag.*, 2016, **11**(1) 5–14. doi: 10.14743/apem2016.1.205
  42. Zaidi, M.G.H.; Joshi, S.K.; Kumar, M.; Sharma, D.; Kumar, A.; Alam, S. & Sah, P.L. Modifications in Mechanical, thermal and electrical characteristics of epoxy through dispersion of multiwalled carbon nanotube in supercritical carbon dioxide. *Carbon Letters*, 2013 **14**(4), 218–227. doi: 10.5714/CL.2013.14.4.218
  43. Joshi, S.K.; Kumar, A.; Mahtab, S. & Zaidi, M.G.H. Modification in mechanical, tribological & electrical Properties of epoxy at low weight fraction of multiwalled carbon nanotube. *In Materials Today Proceeding of 10th International Conference on Materials Processing and Characterization 21st-23rd Feb 2020*: doi: 10.1016/j.matpr.2020.02.394
  44. Xu, D.; Sridhar, V.; Pham, T. T. & Kim, J.K. Dispersion, mechanical and thermal properties of nanographite platelets reinforced fluoroelastomer composites. *e-Polymers*, 2008, no. 023. doi: 10.1515/epoly.2008.8.1.237.
  45. Suherman, H.; Mashyoedin, Y.; Septe, E. & Rizade, R. Properties of graphite/epoxy composites: the in-plane conductivity, tensile strength and Shore hardness. *AIMS Mater. Sci*, 2019, **6**(2), 165–173. doi: 10.3934/matserci.2019.2.165

#### ACKNOWLEDGEMENTS

Research grant funded by Govt. of India. DRDO Letter No CFEES/EVS/B/CAR/024/05 Feb 2015 is hereby acknowledged.

#### CONTRIBUTORS

**Mr Sanjeev Kumar Joshi** has obtained his MSc (Physics) from Kumaun University, Nainital and MTech (CRSE) from G.B. Pant University of Agriculture & Technology, Pant Nagar, Uttarakhand. Currently pursuing his PhD from National Institute of Technology, Kurukshetra, Haryana. Presently working as Scientist ‘F’ and Technology Advisor to Secretary DD R&D and Chairman DRDO with an additional charge of Programme Office (Missiles). His areas of research are CNM composites, computational molecular dynamics, molecular docking, supercritical fluids assisted dispersion of nano-materials, finite element modelling, crack propagation in materials, snow physics and mechanics and avalanche initiation mechanisms. He has more than 30 research publication, technical reports and monograph in his credit.

**Dr M.G.H. Zaidi** is the distinguished Physical Chemist, educator and academic administrator. Presently the Professor and Head, Department of Chemistry, G.B. Pant University of Agriculture & Technology, Pant Nagar, Uttarakhand. His research activities cover the supercritical fluids assisted development of technologically viable polymer materials and their biodegradation. He has published more than 100 research publications, monographs, technical notes in refereed international journals and patents.

**Dr Ashavani Kumar** is working as professor of physics at National Institute of Technology Kurukshetra. He has published more than 100 research papers in international journals, guided more than 70 students for their MTech and PhD degrees; involved as conceptual and reviewer of the work in the paper.